energies

MDPI

Article

Research on Displacement Efficiency by Injecting CO_2 in Shale Reservoirs Based on a Genetic Neural Network Model

Shunli Qin [1], Juhua Li [1,*], Jingyou Chen [1], Xueli Bi [1] and Hui Xiang [2]

[1] Hubei Key Laboratory of Oil and Gas Drilling and Production Engineering, Yangtze University, Wuhan 430100, China
[2] Zhundong Oil Production Plant, Xinjiang Oilfield Company, PetroChina, Fukang 831511, China
* Correspondence: lucyli7509@163.com

Abstract: Carbon dioxide injection can help solve two issues in shale reservoir production. Firstly, it can reduce carbon emissions while, secondly, improving unconventional reservoir recovery. There are many controlling factors for CO_2 injection to enhance oil recovery in shale reservoirs, and the effect of field implementation varies greatly. The key to popularizing this extraction technology is determining the main controlling factors of CO_2 displacement efficiency. Using CO_2 shale displacement laboratory results, the grey correlation analysis method was used to determine the main controlling factors affecting core oil displacement efficiency, such as shale reservoir physical parameters (rock compressibility, porosity, median pore size, matrix permeability, TOC, and oil saturation) and engineering parameters (soaking time and injection pressure). The genetic algorithm (GA) was introduced to optimize the backpropagation (BP) neural network to construct the prediction model of the CO_2 indoor displacement experiments in shale cores. The results showed that the injection pressure among the engineering parameters, the CO_2 soaking time among the gas injection parameters, and the porosity among the shale physical parameters were the main controlling factors affecting the oil displacement efficiency. The prediction accuracy of the genetic neural network model improved, and the coefficient of determination (R^2) reached 0.983. Compared with the conventional neural network model, the mean absolute error (*MAE*) was reduced by 30%, the root mean square error (*RMSE*) was reduced by 46%, and the R^2 increased by 11%. Optimizing the learning and training of the prediction model significantly reduces the cost of laboratory experiments. The deep-learning model completed by training can intuitively show the degree of influence of input parameters on output parameters, providing a theoretical basis for the study of CO_2 displacement mechanisms in shale reservoirs.

Keywords: shale oil; CO_2 fracturing; genetic algorithm; BP neural network; oil displacement efficiency; prediction model

check for updates

Citation: Qin, S.; Li, J.; Chen, J.; Bi, X.; Xiang, H. Research on Displacement Efficiency by Injecting CO_2 in Shale Reservoirs Based on a Genetic Neural Network Model. *Energies* **2023**, *16*, 4812. https://doi.org/10.3390/en16124812

Academic Editors: Shu Tao, Huazhou Huang, Shuoliang Wang and Yanjun Meng

Received: 22 May 2023
Revised: 13 June 2023
Accepted: 14 June 2023
Published: 20 June 2023

Copyright: © 2023 by the authors. Licensee MDPI, Basel, Switzerland. This article is an open access article distributed under the terms and conditions of the Creative Commons Attribution (CC BY) license (https://creativecommons.org/licenses/by/4.0/).

1. Introduction

In recent years, with the development of shale oil and gas exploration, the world has been committed to realizing the scale and efficient development of shale oil and gas reservoirs to alleviate the increasingly severe energy security situation [1]. Unconventional reservoirs are highly heterogeneous, with poor physical properties, diverse reservoir lithologies, and complex pore microstructures [2–4]. Shale oil and gas are stored in micro- and nanopore media, and large-scale volume fracturing using conventional water-based fracturing fluids faces a series of challenges [5]. Utilizing CO_2 fracturing production technology is an effective method to improve shale reservoirs' recovery rates. Compared with water-based fracturing fluid, the advantages of using CO_2 as a fracturing agent are lower fracturing pressure and stronger fracturing ability [6–8]. It can effectively improve the fracture permeability of shale reservoirs and fully utilize the physical and chemical properties of CO_2 (pressure increase, viscosity reduction, dissolution, diffusion, replacement, etc.) to improve the recovery of shale reservoirs [9,10]. In addition, using CO_2 in the extraction

of shale oil reservoirs is conducive to carbon capture, utilization, and storage (CCUS), which reduces environmental pollution, helps reduce carbon emissions on a large scale, and mitigates the greenhouse effect. This technology will be critical in long-term emissions reduction and deep decarbonization [11–13].

Gupta et al. [14,15] classified more than one thousand rock samples from four regions in North America, including Eagle Ford, to study the heterogeneity of shale reservoirs. The recovery enhancement mechanisms and results differed between rock types and fields in the same area. Tovar et al. [16] conducted experiments that involved injecting CO_2 in shale reservoirs to enhance recovery and studied the effects of injection pressure, minimum miscible pressure (MMP), and soaking time on recovery. The experimental results showed that CO_2 could significantly improve the recovery of shale reservoirs. Yu et al. [17] conducted a study on CO_2 injection in tight oil reservoirs to improve recovery, comparing the effect of CO_2 injection on water alternating gas (WAG) and active carbonated water alternating gas (ACWAG) technologies. The results showed that ACWAG achieved the highest recovery rate with CO_2 injection. Several scholars have studied the effect of liquid CO_2 fracturing on unconventional reservoirs. The results showed that CO_2-based fracturing fluids had higher fracturing ability and greater fracture complexity [18–20]. Fracture propagation experiments by supercritical CO_2 (SC-CO_2) fracturing have also been conducted on various shale reservoirs. The results showed that SC-CO_2 fracturing produced more fracture branches than water fracturing. In addition, CO_2 adsorption caused expansion of the shale matrix, which could significantly reduce shale permeability [21,22]. Wu et al. [23] studied the mechanism of CO_2 fracturing throughput in low-permeability reservoirs. The results showed that CO_2 had a better effect on crude oil in terms of solubilization and viscosity reduction, and the degree of CO_2 fracture throughput recovery could reach more than 60%. Zhao et al. [24] conducted a study on the efficiency of CO_2 soaking replacement and replacement of oil and gas in tight reservoirs. The results showed that the replacement efficiency of CO_2 in reservoirs could be effectively improved by increasing the soaking time or improving the reservoir properties.

CO_2 fracturing production technology is still mainly used in indoor experiments and small-scale field trials, such as the Jilin oilfield, the Yanchang oilfield, and the Jimsar shale oilfield in China [25–27]. Due to the small scale of indoor experiments, the high experimental cost, the generally low CO_2 replacement oil displacement efficiency, and the time-consuming and labor-intensive nature of field tests, it is difficult to fully understand and employ experimental results widely in field tests.

As global oil and gas exploration and development become more complex, the demand for technology tends to be refined and enhanced. With its powerful arithmetic and great potential, artificial intelligence has achieved good application results in the oil and gas field [28]. Jiang et al. [29] studied the development trends of intelligent fracturing technologies. They pointed out that using artificial intelligence for the deep mining of small data samples and establishing an integrated fracturing intelligent decision-making platform is conducive to promoting a complete and unified intelligent fracturing technology system. Yang et al. [30] studied optimizing reasonable soaking times in shale reservoirs and established a prediction model based on machine learning. The results showed that the reasonable soaking times calculated by the new model were highly accurate, and the prediction accuracy could reach up to 94% accuracy. Negash et al. [31] conducted artificial-neural-network-based production forecasting for underwater hydrocarbon reservoir injection. The results showed that the proposed fluid production prediction model had a coefficient of determination over 0.9, and the simulation results matched the actual data to a high degree at low computational cost.

Traditional numerical simulation has limitations, such as long modeling times, high computational costs, inaccurate parameter description, and single evaluation effects [32]. Traditional machine-learning algorithms are inadequate regarding computational accuracy, data expansion, and adaptability [28]. As a vital network model for deep learning, the BP

neural network algorithm has a high degree of nonlinear mapping capability, which can avoid the drawbacks of traditional methods [33].

Based on the CO_2 shale core replacement experiments of Tovar et al. [16], this paper introduces a BP neural network optimized by a genetic algorithm to construct a prediction model for indoor replacement experiments to study the effects of numerous parameters involved in CO_2 replacement experiments on replacement efficiency. The goal is to create an understanding of indoor experiments that can be employed in field tests.

2. Data Source and Mechanism Analysis

This study used a BP neural network to analyze the factors affecting the displacement efficiency of shale reservoirs. We introduced a genetic algorithm to optimize the prediction model based on the experimental results for CO_2 throughput displacement shale reservoirs conducted by Tovar et al. [16] The experimental results of small samples could replicate and reproduce themselves and establish the prediction model for CO_2 indoor displacement experiments in shale cores based on the genetic-algorithm-optimized BP neural network to achieve better regularity understanding.

Due to technical limitations, the current recovery rate of North American shale reservoirs is generally between 2% and 16% [34]. Certain achievements have been made in shale reservoirs in the Wolfcamp Formation in North America using CO_2 fracturing production technology, providing a new technical idea for exploiting shale reservoirs [35]. Accordingly, Tovar et al. [16] conducted indoor CO_2 injection displacement experiments in the shale reservoirs of the Wolfcamp Formation, which are rich in organic matter, to explore the differences in the production mechanisms of traditional oil reservoirs. The material used in the experiments was obtained from Wolfcamp shale reservoirs. The cores were 2.5 cm in diameter and ~5 cm in length. Thirteen groups of CO_2 injection displacement experiments of shale cores were carried out to study the influences of physical parameters, injection methods, injection pressure, and soaking time for the different shale reservoirs on the recovery efficiency of shale reservoirs. Three groups of experiments had no test results due to testing errors, and the test data for the remaining 10 groups of displacement experiments are shown in Table 1.

The experiments were sorted according to the MMPs of the injected CO_2 and crude oil. The first four sets of experiments had an MMP of 25.56 MPa for CO_2 and the first fluid sample (crude oil with a density of 0.88 g/cm^3), and the last six sets of experiments had an MMP of 13.28 MPa for CO_2 and the second fluid sample (crude oil with a density of 0.83 g/cm^3). The experimental results focused on the engineering parameters of gas injection, and the influence of gas injection methods, injection pressure, soaking time, and other factors on oil displacement efficiency were discussed in detail, showing:

(i) The effect of gas injection methods. The five groups of core displacement experiments with zero soaking time (experimental serial numbers 3#, 4#, 6#, 9#, and 10#) represented continuous CO_2 injection experiments. The remaining five groups were CO_2 injection throughput experiments represented by different soaking times (reflecting on-site soaking time). The experimental results showed that the oil displacement efficiency of cores with continuous gas injection ranged from 1.7% to 14.7%; the oil displacement efficiency of cores with CO_2 injection throughput ranged from 9.5% to 40%. Overall, it was shown that the replacement process with crude oil in the CO_2 injection throughput of shale cores is the main reason for the higher oil displacement efficiency.

(ii) The effect of injection pressure. Continuous gas injection (zero soaking time) was used for the first fluid sample. Experiments #3 and #4 increased the injection pressure from 17.24 MPa to 24.14 MPa—a pressure increase of 6.9 MPa. The oil displacement efficiency increased from 9.7% to 14.1%—an increase of 4.4 percentage points.

Table 1. The parameters of the displacement experiments on CO_2 injection in shale cores.

Serial Number	Porosity/%	Compressibility/ ($1 \cdot MPa^{-1} \cdot 10^{-3}$)	Oil Saturation/%	MMP/MPa	Crude Oil Density/ ($g \cdot cm^{-3}$)	TOC/wt%	Median Pore Size/nm	Matrix Permeability/nd	Soaking Time/h	Injection Pressure/MPa	Oil Displacement Efficiency/%
1#	10.3	1.18	85.91	25.56	0.88	4.4	7	1370	22	24.14	40
2#	8.22	1.43	30.02	25.56	0.88	2.34	6	530	10	17.24	17.8
3#	5.94	0.93	67.45	25.56	0.88	1.87	5	430	0	17.24	9.7
4#	5.94	0.93	67.45	25.56	0.88	1.87	5	430	0	24.14	14.1
5#	6.44	0.65	50.11	13.28	0.83	2.91	5	370	21	8.28	9.5
6#	10.12	1.27	15.23	13.28	0.83	1.55	5	325	0	14.48	7.4
7#	8.1	0.77	32.22	13.28	0.83	4.08	4	170	21	14.48	14.5
8#	8.65	3.1	65.13	13.28	0.83	3.97	6	390	21	21.38	26.2
9#	7.35	1.33	31.83	13.28	0.83	2.97	5	390	0	8.28	1.7
10#	7.17	1.55	62.7	13.28	0.83	2.18	5	440	0	21.38	14.7

Note: The simulated reservoir temperature was 73.9 °C.

Experiments 6# and 9# with continuous gas injection for the second fluid sample increased the injection pressure from 8.28 MPa to 14.48 MPa. The oil displacement efficiency increased by 5.7 percentage points during the continuous gas injection period. Experiments #5, #7, and #8 using gas injection and throughput with 21 h soaking time showed that when the injection pressure increased from 8.28 MPa to 14.48 MPa (a pressure increase of 6.2 MPa), the oil displacement efficiency increased by 5 percentage points. When the injection pressure increased from 14.48 MPa to 21.38 MPa (a pressure increase of 6.9 MPa), the oil displacement efficiency increased by 11.7 percentage points. The experimental results showed that the injection pressure significantly impacts the oil displacement efficiency. When the pressure is higher than the MMP, the oil displacement efficiency of oil and CO_2 in a miscible state is better.

(iii) The effect of soaking time. For the first fluid sample, experiments 2# and 3# showed that increasing the soaking time from 0 to 10 h at a constant pressure of 17.24 MPa increased the oil displacement efficiency by 8.1 percentage points. Experiments 1# and 4# showed that increasing the soaking time from 0 to 22 h at a pressure of 24.14 MPa increased the oil displacement efficiency by 26 percentage points.

For the second fluid sample, experiments 5#–10# showed that the oil displacement efficiency of soaking throughput increased significantly above that of continuous gas injection at three pressure levels of 8.28 MPa, 14.48 MPa, and 21.38 MPa, regardless of whether the injection pressure was greater or less than the MMP (13.28 MPa). When the injection pressure was less than the MMP, for example, at an injection pressure of 8.28 MPa, the oil displacement efficiency increased nearly five times. When the injection pressure was greater than the MMP (at an injection pressure of 14.48 MPa or 21.38 MPa), the oil displacement efficiency increased by a factor of one.

Due to the limitations of the experimental conditions, indoor experiments can only reflect the oil displacement mechanism under the influence of the experimental factors involved. It is difficult to form a comprehensive understanding of the interrelationship between the experimental factors with a small number of experimental results. They simply cannot be extended to field applications. Additional work is still needed to analyze the relationship between various influencing factors and oil displacement efficiency.

3. Data Processing and Research Methods

3.1. Data Source and Processing

The experimental data in Table 1 were obtained from the CO_2 shale core replacement experimental results of Tovar et al. [16], which contain reservoir geological parameters, crude oil fluid parameters, and injection engineering parameters. The cores used in the experiments were from actual production, so the adopted indoor experimental dataset was representative of the conditions in actual production. To improve the convergence speed of the neural network model and reduce the training error in training, the initial data were normalized before training to normalize the test data to the range of 0~1. The normalization equation is:

$$X_i = \frac{x_i - x_{min}}{x_{max} - x_{min}} \quad (1)$$

where x_i and x_i are the normalized data values and original data values; x_{max} and x_{min} are the maximum and minimum values in the original data.

After integrating the original experimental data and excluding irrelevant data and groups, the cause-free data of the 10 experimental datasets used in this test were obtained, as shown in Table 2.

Table 2. Normalized data.

Serial Number	Porosity/%	Compressibility/ ($1 \cdot MPa^{-1} \cdot 10^{-3}$)	Oil Saturation/%	TOC/wt%	Median Pore Size/nm	Matrix Permeability/nd	Soaking Time/h	Injection Pressure/MPa	Oil Displacement Efficiency/%
1	1.000	0.217	1.000	1.000	1.000	1.000	1.000	1.000	1.000
2	0.523	0.319	0.209	0.277	0.667	0.300	0.455	0.000	0.420
3	0.000	0.115	0.739	0.112	0.333	0.217	0.000	0.000	0.209
4	0.000	0.115	0.739	0.112	0.333	0.217	0.000	1.000	0.324
5	0.115	0.000	0.493	0.477	0.333	0.167	0.955	0.000	0.204
6	0.959	0.250	0.000	0.000	0.333	0.129	0.000	0.473	0.149
7	0.495	0.049	0.240	0.888	0.000	0.000	0.955	0.473	0.334
8	0.622	1.000	0.706	0.849	0.667	0.183	0.955	1.000	0.640
9	0.323	0.277	0.235	0.498	0.333	0.183	0.000	0.000	0.000
10	0.282	0.367	0.672	0.221	0.333	0.225	0.000	1.000	0.339

3.2. Establishment of the BP Neural Network Model

The BP neural network is one of the most widely used neural network models [33]. It is a multilayer feedforward neural network trained according to an error backpropagation algorithm. BP neural networks have the advantages of wide coverage, high adaptability, and good fault tolerance, such that they can overcome the shortcomings of traditional machine-learning algorithms in terms of computational accuracy and adaptability [36]. The topology of the model consists of an input layer, hidden layers, and an output layer. The input and output expressions of the hidden-layer neurons and output-layer neurons are as follows.

$$I_j = \sum_{i=1}^{n} w_{ij} x_i - \theta_j \tag{2}$$

$$O_j = f(I_j) = 1/\left(1 + e^{-I^j}\right) \tag{3}$$

where I_j is the input of the j-th neuron in the hidden or output layer; w_{ij} is the weight of the output from the i-th neuron in the previous layer to the j-th neuron in the hidden or output layer; θ_j is the threshold of the j-th neuron in the hidden or output layer; O_j is the output of the j-th neuron in the hidden or output layer; $f(x)$ is the transfer function; and n is the number of neurons in the previous layer.

As only two groups of fluid samples were selected in this study, corresponding to only two groups of crude oil densities and MMPs, the number of fluid samples would interfere with the ranking of factors. We analyzed the other eight influencing factors using the gray correlation method [37]. Among them, rock compressibility, porosity, TOC, and oil saturation (related to the physical properties of rock reservoirs) reflect the original reserves and decaying recovery capacities in matrix reservoirs. The median pore size reflects the ability of CO_2 to enter the reservoir. The influence of matrix permeability is not significant because the reservoir is put into production by fracturing. The soaking time reflects the degree of CO_2 replacement with crude oil in the reservoir, and the injection pressure reflects the degree of CO_2 mixing phase with crude oil in the reservoir.

The results of the gray correlation analysis are shown in Table 3. In order of correlation, the injection pressure and soaking time among the engineering parameters were the main controlling factors affecting the oil displacement efficiency. The order of influence of the geological parameters, from greatest to least, was: porosity, median pore size, TOC, compressibility, oil saturation, matrix permeability. Finally, the first seven indexes with a correlation higher than 0.95 were selected as the input-layer parameters of the BP neural network, and the oil displacement efficiencies of the indoor experiments were selected as the output-layer parameters to establish the prediction model for the shale core CO_2 indoor displacement experiments based on the BP neural network.

Table 3. The results of the analysis of the degree of correlation between various influencing factors and oil displacement efficiency.

Evaluation Items	Relevance	Ranking
Injection pressure/MPa	0.991	1
Soaking time/h	0.986	2
Porosity/%	0.986	3
Median pore size/nm	0.984	4
TOC/wt%	0.981	5
Compressibility/(1·MPa^{-1}·10^{-3})	0.979	6
Oil saturation/%	0.95	7
Matrix permeability/nd	0.615	8

The parameters through the input layer were divided into each hidden layer, and each hidden-layer node then performed operations, such as the encoding of weights and thresholds and error evaluation for each input datum. In turn, the output result was obtained: the indoor experimental oil displacement efficiency obtained from this training and prediction. The single-layer structure was chosen for the hidden layer of the BP neural network of this model, and the number of nodes in the hidden layer was obtained by the empirical Equation (4), and the error was smaller when the number of nodes in the hidden layer was 10. The BP neural network structure diagram for the prediction model for the indoor displacement experiments is shown in Figure 1.

$$p = \sqrt{m+n} + q \tag{4}$$

where p is the number of nodes in the hidden layers; n is the number of nodes in the input layer; m is the number of nodes in the output layer; and q is an integer between 1 and 10.

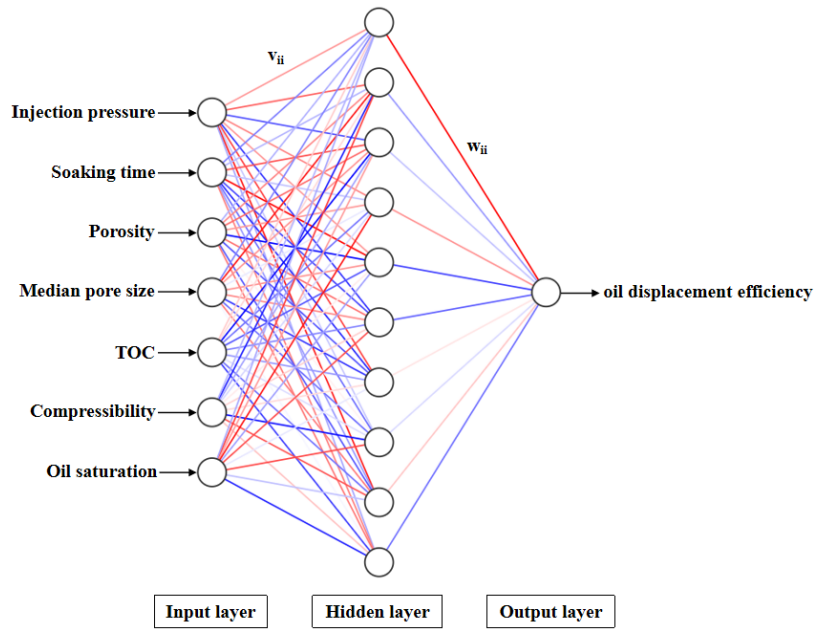

Figure 1. BP neural network structure diagram for the prediction model for the indoor displacement experiments. (The v_{ii} in the figure denotes the connection weight between the input layer and the hidden layers of the BP neural network, and w_{ii} denotes the connection weight between the hidden layers and the output layer.)

3.3. Establishment of the BP Neural Network Model Optimized by a Genetic Algorithm

The traditional BP neural network algorithm has several problems, including slow convergence, poor searching ability, and the fact that it easily falls into local minima, which

are disadvantages in training [38]. The genetic algorithm (GA) has good optimization ability regarding the initial weights and thresholds of the BP neural network, and the optimized model quickly converges and has a low computational cost [39]. Considering the small sample of the dataset for this research object, we introduced the genetic algorithm to optimize and improve the BP neural network, constructed the prediction model for the shale core CO_2 indoor displacement experiments based on the GA-BP neural network, and then laid the material foundation for the indoor experiments to guide field applications.

The structure of the model mainly includes two parts: the BP neural network and the genetic algorithm optimization [40]. First, regarding the BP neural network, the parameters and states of the input, hidden, and output layers are determined; the topology of the network model is established; and then the weights and thresholds are initialized. The genetic algorithm optimization encodes the weights and thresholds from the BP neural network; performs genetic selection, crossover, and variation operations to obtain the fitness results; and feeds the optimal weights and thresholds back to the neural network. The fitness function is shown in Equation (5). Finally, the BP neural network is continuously trained and evaluated until it meets the target requirements for prediction and output. The GA-BP neural network algorithm flow of the prediction model is shown in Figure 2.

$$A_{(i)} = \frac{1}{\sum_{i=1}^{n}(\hat{y}(i) - y(i))^2} \tag{5}$$

where n is the number of samples; $\hat{y}(i)$ and $y(i)$ are the simulated values and actual values of sample i.

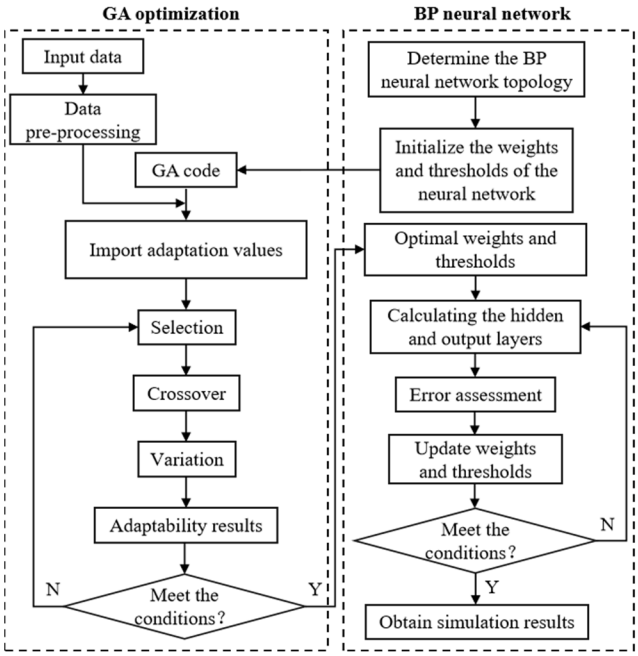

Figure 2. The GA-BP neural network algorithm flow of the prediction model.

In this study, Matlab software was used for programming. Ten sets of dataset samples were divided into training and testing sets (the first six sets were training samples, and the last four sets were testing samples) to train and test the neural network model. In training, the maximum number of iterations for the BP neural network training was set to 1000, the error threshold was 1×10^{-6}, and the learning rate was 0.01. The number of genetic generations for genetic algorithm optimization was set to 50, the population size was 10, the crossover probability was 0.7, and the variation probability was 0.1.

3.4. Evaluation Indicators

To comprehensively evaluate the accuracy of the model, the mean absolute error (*MAE*), root mean square error (*RMSE*), and coefficient of determination (R^2) were calculated to evaluate the accuracy of the experimental prediction model of shale core replacement. The smaller the values for *MAE* and *RMSE*, the smaller the model error; and the closer the value of the coefficient of determination R^2 is to 1, the better the model fit. The specific formulas for the evaluation indicators are as follows.

$$MAE = \frac{1}{n}\sum_{i=1}^{n}|y_i - y_i'| \tag{6}$$

$$RMSE = \sqrt{\frac{1}{n}\sum_{i=1}^{n}(y_i - y_i')^2} \tag{7}$$

$$R^2 = 1 - \frac{\sum_{i=1}^{n}(y_i - y_i')^2}{\sum_{i=1}^{n}(y_i - \overline{y})^2} \tag{8}$$

where y_i and y_i' are the actual and predicted values of oil displacement efficiency (%); $\overline{y}$ is the arithmetic mean of the actual values of oil displacement efficiency; and n is the number of samples.

4. Results and Discussion

4.1. The BP Neural Network Model Testing

After data processing, parameter fitting, and error evaluation, the BP neural network prediction model obtained from the training set was used to predict the last four sets. The fitting results for the oil displacement efficiency are shown in Figure 3. The comparison shows that the predicted trend of shale core displacement agrees with the actual values. The comparison in Figure 3a,b shows that the model fits the training set better than it predicts the testing set. Figure 3a shows that the BP neural network model has a better fit to the three sets of training data with low oil displacement efficiency (experiments #4, #5, and #6) because the conventional BP neural network model is insensitive to changes in parameters that affect the oil displacement efficiency. When the parameters fluctuate within a certain range, the BP neural network model tends to have better prediction results.

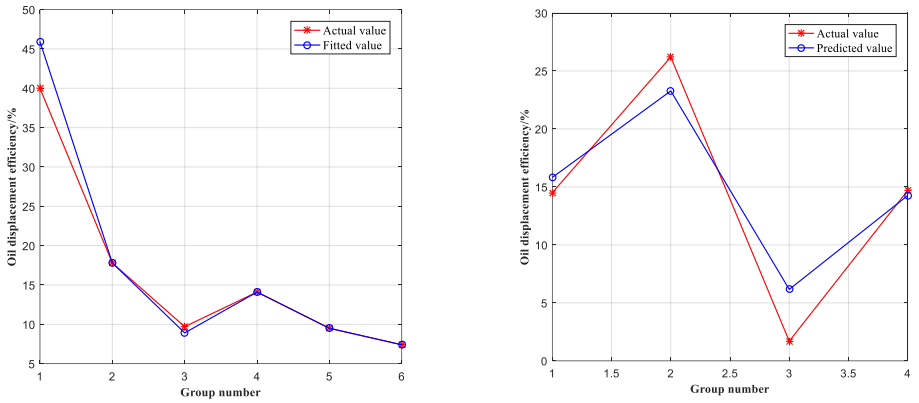

(**a**) (**b**)

Figure 3. Comparison of fitting results of the shale core displacement experiments based on the BP neural network: (**a**) comparison of the fitted values and the actual values; (**b**) comparison of the predicted values and the actual values.

The prediction accuracy of the BP neural network model is shown in Table 4. The mean absolute error of the prediction set is 1.286, the root mean square error is 1.757, and

the R^2 is 0.899. The overall experimental results show that the results for the traditional BP neural network model trained on the first six groups of samples were not better applied to the prediction of the last four groups of samples.

Table 4. Comparison of oil displacement efficiency prediction effects and errors based on the BP neural network and the GA-BP neural network.

Model Type	Predicted Group Number	Actual Value/%	Predicted Value/%	*MAE*	*RMSE*	R^2
BP model	1	14.50	15.82	1.286	1.757	0.889
	2	26.20	23.28			
	3	1.70	5.86			
	4	14.70	14.26			
GA-BP model	1	14.50	14.64	0.898	0.946	0.983
	2	26.20	26.49			
	3	1.70	2.81			
	4	14.70	15.85			

4.2. Model Testing and Analysis after Optimization by the Genetic Algorithm

After the genetic algorithm optimization of the above BP neural network model, the GA-BP neural network prediction model obtained from the training was used again to predict the last four groups of samples. The fitness curve of the optimized prediction model is shown in Figure 4. It can be seen that the individual adaptation index gradually decreases and that the adaptation ability gradually increases after the multiple optimization and calculation of the GA-BP neural network model. When the number of iterations reaches 29, the individual adaptation level gradually stabilizes.

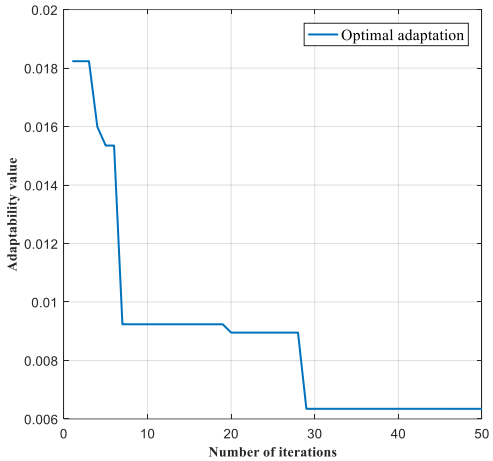

Figure 4. The fitness curve of the GA-BP neural network prediction model.

The comparison of the fitting results for oil displacement efficiency obtained after optimization is shown in Figure 5. The predicted values of the BP neural network prediction model optimized by the genetic algorithm fit better with the actual values. The GA-BP neural network model improved the fitting effect of the first two training sets. Due to the selection and iteration of genetic variants, the accuracy of the model was improved. The results show that the BP neural network prediction model optimized by the genetic algorithm improved the sensitivity to the data compared to the BP neural network. The predicted results in Figure 5b show that the magnitude of injection pressure is positively correlated with the predicted oil displacement efficiency. Soaking time has a greater degree of influence on the model. The soaking time enhances the degree of CO_2 replacement with crude oil under the condition that other influencing factors remain unchanged. Under

certain conditions and with the same injection pressure, the longer the soaking time, the higher the predicted oil displacement efficiency obtained (experiments 8# and 10#).

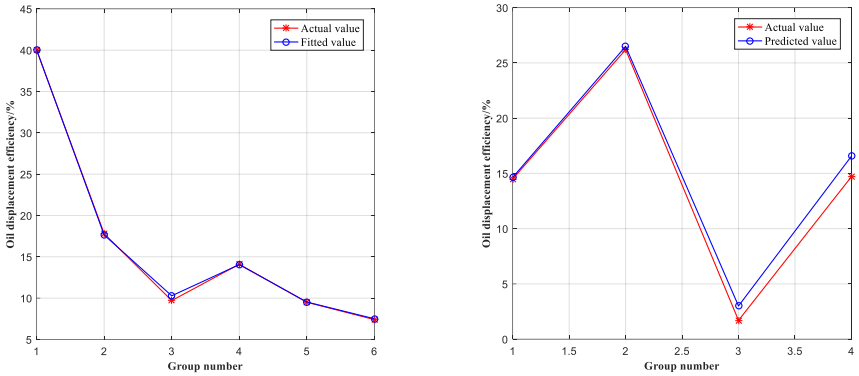

(**a**) (**b**)

Figure 5. Comparison of fitting results of the shale core displacement experiments based on the GA-BP neural network: (**a**) comparison of the fitted values and the actual values; (**b**) comparison of the predicted values and the actual values.

The prediction accuracy of the GA-BP neural network model is shown in Table 4. The results show that the accuracy of the predicted values of the GA-BP neural network model improved, with a mean absolute error of 0.898, a root mean square error of 0.946, and the R^2 reaching 0.983. After optimization by the genetic algorithm, the mean absolute error was reduced by 30%, the root mean square error was reduced by 46%, and the R^2 increases by 11%.

4.3. Application of the Method

The prediction model based on the GA-BP neural network constructed for shale core CO_2 indoor replacement experiments can be used to examine the effects of various influencing factors on oil displacement efficiency under different experimental conditions. The experimental fluid sample density was 0.83 g/cm^3, the experimental temperature was 73.9 °C, the corresponding MMP was 13.28 MPa, and multiple sets of prediction experiments were designed. The injection pressures were 7 MPa, 15 MPa, and 20 MPa. The soaking times were 0, 10 h, and 25 h. The other experimental conditions were set within a reasonable range, and the specific test data are shown in Table 5.

Table 5. The test data for the prediction experiment.

Serial Number	Porosity/%	Compressibility/ ($1 \cdot MPa^{-1} \cdot 10^{-3}$)	Oil Saturation/%	TOC/wt%	Median Pore Size/nm	Soaking Time/h	Injection Pressure/MPa
1	7.65	0.98	67.45	3.18	4	25	15
2	5.86	1.43	34.45	1.78	5	0	15
3	7.76	1.67	55.67	2.87	5	10	7
4	6.96	1.24	68.9	1.56	4	0	7
5	10.2	1.52	89.65	2.41	6	25	20
6	8.46	1.14	77.4	3.8	5	10	15
7	8.28	1.2	35.78	2.65	6	25	7
8	7.66	2.3	62.8	2.21	5	10	20
9	9.65	1.16	40.69	2.32	5	0	20

The GA-BP neural network indoor displacement experimental prediction model was subjected to data processing, parameter fitting, and error evaluation. The results of this prediction experiment were obtained, as shown in Figure 6. The mean absolute error, root mean square error, and R^2 of the test set highlight the high accuracy of the model. The predicted oil displacement efficiency results are within a reasonable range. The analysis of the prediction results shows that the experimental pattern of the effect of gas injection methods, injection pressure, and soaking time on oil displacement efficiency is in remarkable

agreement with the indoor experiments on core displacement of Tovar et al. [16]. Overall, the accuracy of the prediction results of the GA-BP neural network prediction model is high, and the model is suitable for experimental modeling.

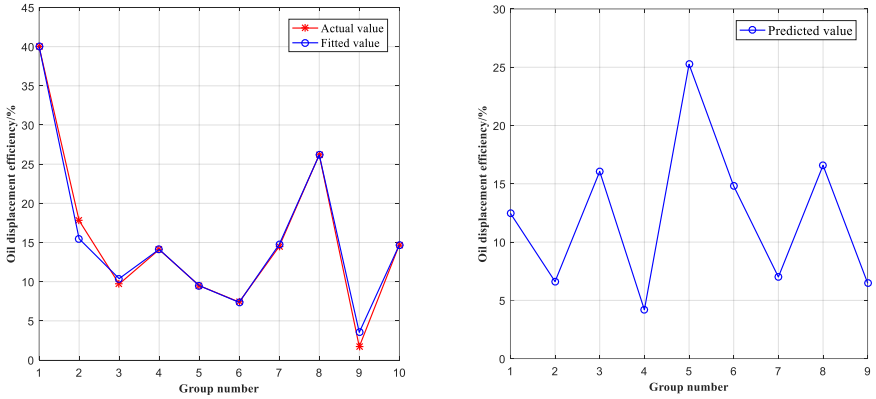

(**a**) (**b**)

Figure 6. The prediction experiment results based on the GA-BP neural network: (**a**) comparison of the fitted values and the actual values; (**b**) the predicted values for oil displacement efficiency.

5. Conclusions

(i) The factors influencing oil displacement efficiency were ranked using gray correlation analysis based on shale core CO_2 displacement experiments and parameters. Numerous constraining factors influence oil recovery in the integrated development process of CO_2 soaking production in shale reservoirs and the significant variation in the field implementation effect. The findings demonstrated that the main controlling factors affecting oil displacement efficiency are the injection pressure, the CO_2 soaking time, and the reservoir porosity.

(ii) This paper established a genetic-algorithm-optimized-BP-neural-network-based prediction model for CO_2 indoor displacement experiments on shale cores. Compared with the traditional BP neural network prediction model, the fitting degree and prediction accuracy of the GA-BP neural network prediction model were enhanced. The mean absolute error was reduced by 30%, the root mean square error was reduced by 46%, and the R^2 increased by 11%. This provides a theoretical basis for the indoor experimental study of CO_2 oil displacement mechanisms.

(iii) The model optimized by the genetic algorithm overcomes the slow convergence problems, poor searching ability, and the tendency to fall into local minima exhibited by traditional neural networks. In practical production, the model can play an important role in prediction and evaluation by learning various types of dynamic and static influencing factors and overcoming the above issues with previous models while reducing experimental costs.

(iv) The factors affecting the actual oil displacement efficiency in shale reservoirs are complex and diverse. In actual production, CO_2 injection methods, actual injection pressure, and CO_2 soaking time have a huge impact on the oil displacement efficiency. Due to the small number of samples and algorithmic flaws, the present model still has some limitations, and needs to be fully trained and improved. More experimental or field samples should be acquired in the future, and better BP neural network algorithms should be sought to further the application of this prediction model.

Author Contributions: Conceptualization, S.Q.; methodology, S.Q.; software, S.Q. and J.C.; investigation, S.Q., J.C. and X.B.; data curation, S.Q., J.C. and H.X.; resources, S.Q., J.L. and H.X.; writing—original draft preparation, S.Q.; writing—review and editing, S.Q., J.L., J.C., X.B. and H.X.; supervision, J.L.; funding acquisition, J.L. and H.X. All authors have read and agreed to the published version of the manuscript.

Funding: This work is financially supported by the Major National Science and Technology Projects of China (No. 2016ZX05060-019).

Data Availability Statement: The data source has been explained in the article.

Conflicts of Interest: The authors declare no conflict of interest.

References

1. Liu, H.; Tao, J.; Meng, S.; Li, D.; Cao, G.; Gao, Y. Application and prospects of CO_2 enhanced oil recovery technology in shale oil reservoir. *J. China Pet. Explor.* **2022**, *27*, 127–134.
2. Wang, Y.; Lv, Z. Composite stimulation technology for improving fracture length and conductivity of unconventional reservoirs. *J. Front. Phys.* **2023**, *11*, 371. [CrossRef]
3. Tsiglianu, P.; Romasheva, N.; Nenko, A. Conceptual Management Framework for Oil and Gas Engineering Project Implementation. *J. Resour.* **2023**, *12*, 64. [CrossRef]
4. Martirosyan, A.V.; Kukharova, T.V.; Fedorov, M.S. Research of the Hydrogeological Objects' Connection Peculiarities. In Proceedings of the 2021 IV International Conference on Control in Technical Systems (CTS), St. Petersburg, Russia, 21–23 September 2021; IEEE: Piscataway, NJ, USA, 2001; pp. 34–38.
5. Wu, D.; Geng, Y.; Xiao, X.; Miao, F.; Zhai, W. Experimental study on variation pattern of enhanced permeability of supercritical CO_2 in shale reservoirs. *J. Spec. Oil Gas Reserv.* **2022**, *29*, 66–72.
6. Li, N.; Yu, J.; Wang, C.; Zhang, S.; Liu, X.; Kang, J.; Wang, Y.; Dai, Y. Fracturing technology with carbon dioxide: A review. *J. Pet. Sci. Eng.* **2021**, *205*, 108793.
7. Pu, W.; Du, D.; Wang, S.; Zeng, L.; Feng, R.; Memon, S.; Sarout, J.; Varfolomeev, M.A.; Sarmadivaleh, M.; Xie, Q. Experimental study of CO_2 huff-n-puff in a tight conglomerate reservoir using true triaxial stress cell core fracturing and displacement system: A case study. *J. Pet. Sci. Eng.* **2021**, *199*, 108298. [CrossRef]
8. Li, S.; Zhang, S.; Zou, Y.; Ma, X.; Ding, Y.; Li, N.; Zhang, X.; Kasperczyk, D. Pore structure alteration induced by CO_2–brine–rock interaction during CO_2 energetic fracturing in tight oil reservoirs. *J. Pet. Sci. Eng.* **2020**, *191*, 107147. [CrossRef]
9. Zhang, X.; Lu, Y.; Tang, J.; Zhou, Z.; Liao, Y. Experimental study on fracture initiation and propagation in shale using supercritical carbon dioxide fracturing. *Fuel* **2017**, *190*, 370–378. [CrossRef]
10. Zhang, C.; Cheng, P.; Ranjith, P.G.; Lu, Y.; Zhou, J. A comparative study of fracture surface roughness and flow characteristics between CO_2 and water fracturing. *J. Nat. Gas Sci. Eng.* **2020**, *76*, 103188. [CrossRef]
11. Sher, F.; Iqbal, S.Z.; Albazzaz, S.; Ali, U.; Mortari, D.A.; Rashid, T. Development of biomass derived highly porous fast adsorbents for post- combustion CO_2 capture. *Fuel* **2020**, *282*, 118506. [CrossRef]
12. Qureshi, Y.; Ali, U.; Sher, F. Part load operation of natural gas fired power plant with CO_2 capture system for selective exhaust gas recirculation. *J. Appl. Therm. Eng.* **2021**, *190*, 116808. [CrossRef]
13. Yuan, S.; Ma, D.; Li, J.; Zhou, T.; Ji, Z.; Han, H. Progress and prospects of carbon dioxide capture, EOR-utilization and storage industrialization. *J. Pet. Explor. Dev.* **2022**, *49*, 828–834. [CrossRef]
14. Gupta, I.; Rai, C.; Sondergeld, C.; Devegowda, D. Rock typing in Wolfcamp formation. In Proceedings of the SPWLA 58th Annual Logging Symposium, Oklahoma City, OK, USA, 17–21 June 2017.
15. Gupta, I.; Rai, C.; Sondergeld, C.; Devegowda, D. Rock Typing in Eagle Ford, Barnett, and Woodford Formations. *J. SPE Reserv. Eval. Eng.* **2018**, *21*, 654–670. [CrossRef]
16. Tovar, F.D.; Barrufet, M.A.; Schechter, D.S. Enhanced oil recovery in the wolfcamp shale by carbon dioxide or nitrogen injection: An experimental investigation. *SPE J.* **2021**, *26*, 515–537. [CrossRef]
17. Yu, H.; Fu, W.; Zhang, Y.; Lu, X.; Cheng, S.; Xie, Q.; Qu, X.; Yang, W.; Lu, J. Experimental study on EOR performance of CO_2-based flooding methods on tight oil. *Fuel* **2021**, *290*, 119988. [CrossRef]
18. Ma, D.; Cheng, C.; Ding, C.; Song, J.; Hu, D.; Zhou, H. Comparisons of fracturing mechanism of tight sandstone using liquid CO_2 and water. *J. Nat. Gas Sci. Eng.* **2021**, *94*, 104108. [CrossRef]
19. Yang, B.; Wang, H.; Wang, B.; Shen, Z.; Zheng, Y.; Jia, Z.; Yan, W. Digital quantification of fracture in full-scale rock using micro-CT images: A fracturing experiment with N_2 and CO_2. *J. Pet. Sci. Eng.* **2021**, *196*, 107682. [CrossRef]
20. Liao, Z.; Liu, X.; Song, D.; He, X.; Nie, B.; Yang, T.; Wang, L. Micro-structural damage to coal induced by liquid CO_2 phase change fracturing. *J. Nat. Resour. Res.* **2021**, *30*, 1613–1627. [CrossRef]
21. Zhou, J.; Liu, G.; Jiang, Y.; Xian, X.; Liu, Q.; Zhang, D.; Tan, J. Supercritical carbon dioxide fracturing in shale and the coupled effects on the permeability of fractured shale: An experimental study. *J. Nat. Gas Sci. Eng.* **2016**, *36*, 369–377. [CrossRef]
22. Zhao, Z.; Li, X.; He, J.; Mao, T.; Zheng, B.; Li, J. A laboratory investigation of fracture propagation induced by supercritical carbon dioxide fracturing in continental shale with interbeds. *J. Pet. Sci. Eng.* **2018**, *166*, 739–746. [CrossRef]
23. Wu, J.; Liu, B.; Liu, D.; Wang, C.; Li, Y.; Liu, G. Test of CO_2 miscible fracturing and huff and puff. *J. Spec. Oil Gas Reserv.* **2022**, *29*, 126–131.
24. Zhao, Q.; Jiang, H.; Meng, W.; Wang, J.; Wang, C.; Xiu, H. Experimental study on replacement efficiency of carbon dioxide in tight oil and gas reservoirs. *J. Nat. Gas Geosci.* **2021**, *32*, 718–726.
25. Zhang, H.; Yu, X.; Ma, L.; Chen, G.; Zheng, X.; Zhao, S. Potentials of the gas flooding for Jilin low-permeability oil reservoirs. *J. Pet. Geol. Oilfield Dev. Daqing* **2014**, *33*, 130–134.

26. Wang, X.; Yang, H.; Wang, W.; Li, J.; Liang, Q. Technical advancements in enhanced oil recovery in low permeability reservoirs of Yanchang Oilfield. *J. Pet. Geol. Recovery Effic.* **2022**, *29*, 69–75.
27. Tang, W.; Huang, Z.; Chen, C.; Ding, Z.; Sheng, J.; Wang, X.; Le, P. Optimization of CO_2 huff and puff scheme for Jimsar shale oil and evaluation of test effect. *J. Spec. Oil Gas Reserv.* **2022**, *29*, 131–137.
28. Min, C.; Dai, B.; Zhang, X.; Du, J. A Review of application progress of machine learning in oil and gas industry. *J. Southwest Pet. Univ. (Sci. Technol. Ed.)* **2020**, *42*, 1–15.
29. Jiang, T.; Zhou, J.; Liao, L. Development status and future trends of intelligent fracturing technologies. *J. Pet. Drill. Tech.* **2022**, *50*, 1–9.
30. Yang, H.; Xue, M.; Yang, Y.; Ma, L.; Feng, Z. Prediction of reasonable soaking time of oil wells in shale reservoir based on machine learning methods. *J. Xi'an Shiyou Univ. (Nat. Sci. Ed.)* **2022**, *37*, 65–72.
31. Negash, B.M.; Yaw, A.D. Artificial neural network based production forecasting for a hydrocarbon reservoir under water injection. *J. Pet. Explor. Dev.* **2020**, *47*, 357–365. [CrossRef]
32. Lei, Z.; Xin, X.; Yu, G.; Wang, L. Reservoir Production Performance Optimization Algorithm Based on Numerical Simulation. *J. Xinjiang Pet. Geol.* **2022**, *43*, 612–616.
33. Zhu, D.; Shi, H. *Principle and Application of Artificial Neural Network*; Beijing Science Press: Beijing, China, 2006; pp. 166–168.
34. Delaihdem, D.K. *Decline Curve Analysis and Enhanced Shale Oil Recovery Based on Eagle Ford Shale Data*; University of Alaska Fairbanks: Fairbanks, AK, USA, 2013; pp. 186–205.
35. Loucks, R.G.; Reed, R.M.; Ruppel, S.C.; Jarvie, D.M. Morphology, Genesis, and Distribution of Nanometer-Scale Pores in Siliceous Mudstones of the Mississippian Barnett Shale. *J. Sediment. Res.* **2009**, *79*, 848–861. [CrossRef]
36. Zhou, Y.; Liu, H.; Qi, P.; Zhao, M.; Chen, Y. Forecast of oil production in fractured-vuggy reservoir by using recurrent neural networks. *Chin. J. Comput. Phys.* **2018**, *35*, 668–674.
37. Liu, S.; Cai, H.; Yang, Y.; Cao, Y. Advance in grey incidence analysis modelling. *Syst. Eng. Theory Pract.* **2013**, *33*, 2041–2046.
38. Liu, W.; Liu, S.; Bai, R.; Zhou, X.; Zhou, D. Research of mutual learning neural network training method. *Chin. J. Comput.* **2017**, *40*, 1291–1308.
39. Yu, S. *MATLAB Optimization Algorithm Case Analysis and Application: Advanced Chapter*; Tsinghua University Press: Beijing, China, 2015; pp. 124–126.
40. Huang, J.; Luo, H.; Wang, H.; Long, B. Prediction of time sequence based on GA-BP neural net. *J. Univ. Electron. Sci. Technol. China* **2009**, *38*, 687–692.

Disclaimer/Publisher's Note: The statements, opinions and data contained in all publications are solely those of the individual author(s) and contributor(s) and not of MDPI and/or the editor(s). MDPI and/or the editor(s) disclaim responsibility for any injury to people or property resulting from any ideas, methods, instructions or products referred to in the content.